Northward extent of East Asian monsoon covaries with intensity on orbital and millennial timescales

Yonaton Goldsmith[a,1], Wallace S. Broecker[a], Hai Xu[b,1], Pratigya J. Polissar[a], Peter B. deMenocal[a], Naomi Porat[c], Jianghu Lan[b], Peng Cheng[b], Weijian Zhou[b], and Zhisheng An[b]

[a]Lamont–Doherty Earth Observatory, Columbia University, Palisades, NY 10964; [b]State Key Laboratory of Loess and Quaternary Geology, Institute of Earth Environment, Chinese Academy of Sciences, Xi'an 710061, Shaanxi, China; and [c]Geological Survey of Israel, Jerusalem 95501, Israel

Edited by Jeffrey P. Severinghaus, Scripps Institution of Oceanography, La Jolla, CA, and approved December 28, 2016 (received for review October 7, 2016)

The magnitude, rate, and extent of past and future East Asian monsoon (EAM) rainfall fluctuations remain unresolved. Here, late Pleistocene–Holocene EAM rainfall intensity is reconstructed using a well-dated northeastern China closed-basin lake area record located at the modern northwestern fringe of the EAM. The EAM intensity and northern extent alternated rapidly between wet and dry periods on time scales of centuries. Lake levels were 60 m higher than present during the early and middle Holocene, requiring a twofold increase in annual rainfall, which, based on modern rainfall distribution, requires a ∼400 km northward expansion/migration of the EAM. The lake record is highly correlated with both northern and southern Chinese cave deposit isotope records, supporting rainfall "intensity based" interpretations of these deposits as opposed to an alternative "water vapor sourcing" interpretation. These results indicate that EAM intensity and the northward extent covary on orbital and millennial timescales. The termination of wet conditions at 5.5 ka BP (∼35 m lake drop) triggered a large cultural collapse of Early Neolithic cultures in north China, and possibly promoted the emergence of complex societies of the Late Neolithic.

East Asian monsoon | closed-basin lake | paleo-rainfall | Chinese cave record | northward expansion

The East Asian monsoon (EAM) is a major component of the global climate system (1), and its variability directly impacts the lives of over a billion people. Understanding EAM sensitivity to past climate changes and its future variability are essential for determining the EAM response to different climate forcings and for constraining future climate projections. Two competing interpretations of existing paleoclimate records frame our current understanding of the response of the EAM to orbital-scale and high-latitude millennial-scale forcing during the late Pleistocene–Holocene. The first interpretation suggests that oxygen isotopic records from Chinese cave deposits reflect real rainfall changes, indicating a direct response of EAM rains to external climate forcings (2–4). The competing view holds that these isotopic records reflect changes in moisture sourcing and depend on the Indian Monsoon intensity (5–10), suggesting that the cave deposit isotopic values are decoupled from actual rainfall amounts, and thus question the validity of oxygen isotope–based EAM intensity reconstructions. Missing from this debate has been an independent quantitative record of past rainfall variability in the EAM region.

Here, we present a detailed, well-dated lake-level history for Lake Dali (43.15°N, 116.29°E), a closed-basin lake in Inner Mongolia (1,220 m above sea level, 220 km^2 lake area and maximum depth of 11 m), presently located near the northwestern limit of EAM domain (e.g., ref. 11; Fig. 1). The peripheral location of Lake Dali with respect to the monsoon region provides an excellent opportunity to examine the magnitude of spatial expansion of the EAM and whether the millennial- and orbital-scale changes observed in Chinese cave deposit records were accompanied by real changes in monsoonal rainfall.

Closed-basin lakes are, to first order, controlled by the amount of rainfall that falls in the catchment of a lake, and thus are powerful recorders of past changes in annual rainfall amounts (12). Lake Dali Lake-level record is unique because closed basin lakes are scarce in the EAM region (13), and thus this record is an independent proxy for the EAM precipitation amount and a benchmark for interpreting the seminal Chinese cave records.

Modern rainfall in Lake Dali occurs during the warm boreal summer (June to September), whereas during boreal winter temperatures drop and the lake freezes over. Local rainfall seasonality and long-term variability are representative of the EAM in northern China (*SI Materials and Methods*; Fig. S1). Therefore, the water budget of Lake Dali should be sensitive to regional precipitation shifts in northern China and thus reflect EAM fluctuations.

Lake beach ridges and sediment outcrops observed above the modern lake level represent past variations of lake-level elevation and extent. Satellite images and an advanced spaceborne thermal emission and reflection radiometer (ASTER) digital elevation model (DEM; 30-m resolution) were used to locate and map these shoreline markers. In the field, 41 sediment outcrops and beach ridges were mapped and stratigraphic relations were evaluated (Fig. S2). Thirty-six radiocarbon ages were obtained from aquatic shells and charcoal (reported as calibrated calendar ages before present [BP]) and nine optical stimulated luminescence (OSL) samples were measured. Radiocarbon measurements of modern lake and river water dissolved inorganic carbon and a submerged aquatic plant indicate that currently the lake water is at radiocarbon equilibrium with the atmosphere (*SI Materials and Methods* and Table S1), obviating the need for a reservoir correction. The local geology is composed of Jurassic granite, late Pleistocene basalt, and Quaternary sand dunes (14). The absence of limestone in the catchment of the lake also minimizes possible introduction of old radiocarbon into the lake.

Significance

The magnitude, rate, and extent of past and future East Asian monsoon (EAM) rainfall fluctuations remain unresolved. Here, we present a rainfall reconstruction based on the surface area of a closed-basin lake located at the modern northwestern boundary of the EAM. Our record shows that fluctuations of EAM intensity and spatial extent covaried over the past 125 ka. This record contributes to the resolution of a current controversy concerning the response of the EAM to external climatic forcings. We propose that a substantial decrease in rainfall at 5.5 ka was a major factor leading to a large cultural collapse of the Early Neolithic culture in north China.

Author contributions: Y.G., W.S.B., P.J.P., P.B.d., and Z.A. designed research; Y.G., W.S.B., H.X., P.J.P., N.P., and J.L. performed research; Y.G., W.S.B., P.J.P., P.B.d., and W.Z. contributed new reagents/analytic tools; Y.G., W.S.B., H.X., P.J.P., P.B.d., N.P., P.C., and W.Z. analyzed data; and Y.G., W.S.B., H.X., P.J.P., P.B.d., N.P., and Z.A. wrote the paper.

The authors declare no conflict of interest.

This article is a PNAS Direct Submission.

[1]To whom correspondence may be addressed. Email: yonig@ldeo.columbia.edu or xuhai@ieecas.cn.

This article contains supporting information online at www.pnas.org/lookup/suppl/doi:10.1073/pnas.1616708114/-/DCSupplemental.

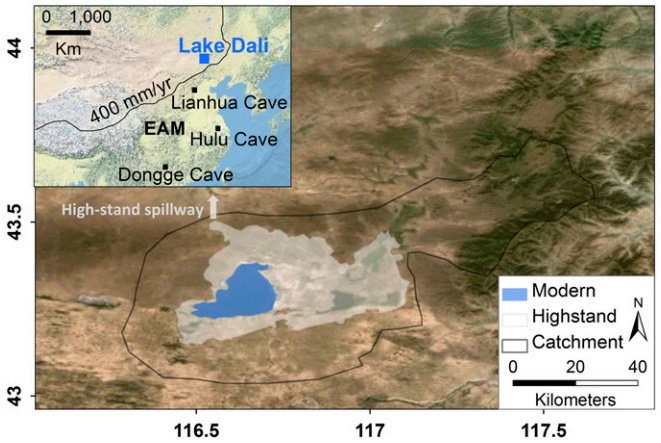

Fig. 1. Modern and highstand extent and catchment of Lake Dali. *Inset* shows extent of the EAM (30) and the location of Lake Dali and Lianhua, Hulu, and Dongge caves.

Results

The results show that the lake fluctuated on both orbital and millennial time scales. The lake reached highstands at 123 ± 13 ka (marine isotope stage 5e), 58 ± 5 ka (between marine isotope stages 3 and 4), and 11–5.5 ka (marine isotope stage 1) (Figs. 2 and 3). These three major highstands occurred during periods of high boreal summer insolation, indicating that the intensity/extent of the EAM is governed by summer insolation intensity. Erosion and burial result in scarce pre-Holocene shoreline evidence; therefore, additional highstands cannot be excluded.

During the Late Glacial (16–11.5 ka) the lake fluctuated on millennial time scales, with the Bølling–Allerød (B–A) and Younger Dryas periods having high and low lake levels, respectively (Fig. 2). These abrupt fluctuations occurred during times of relatively low insolation and are coeval with Greenland and circum-North Atlantic records, indicating that the EAM responded to climatic forcings that originated in the North Atlantic through teleconnections most likely related to shifts in the position of the thermal equator (15) and the associated shifts in the westerlies position (10).

Lake levels during the Early and Middle Holocene were overall high, corresponding to the Early Middle Holocene summer (June–August; JJA) insolation maxima. The onset (~60 m rise in 400 y) and termination (~35 m drop in 1 ka) of the Holocene humid period occurred rapidly. During four intervals in the Early and Middle Holocene (11.5–11, 10.5–9.5, 8.3–7.8, and 6.1–5.9 ka), lake levels were particularly high, with lake drops occurring between these intervals. These millennial fluctuations appear in

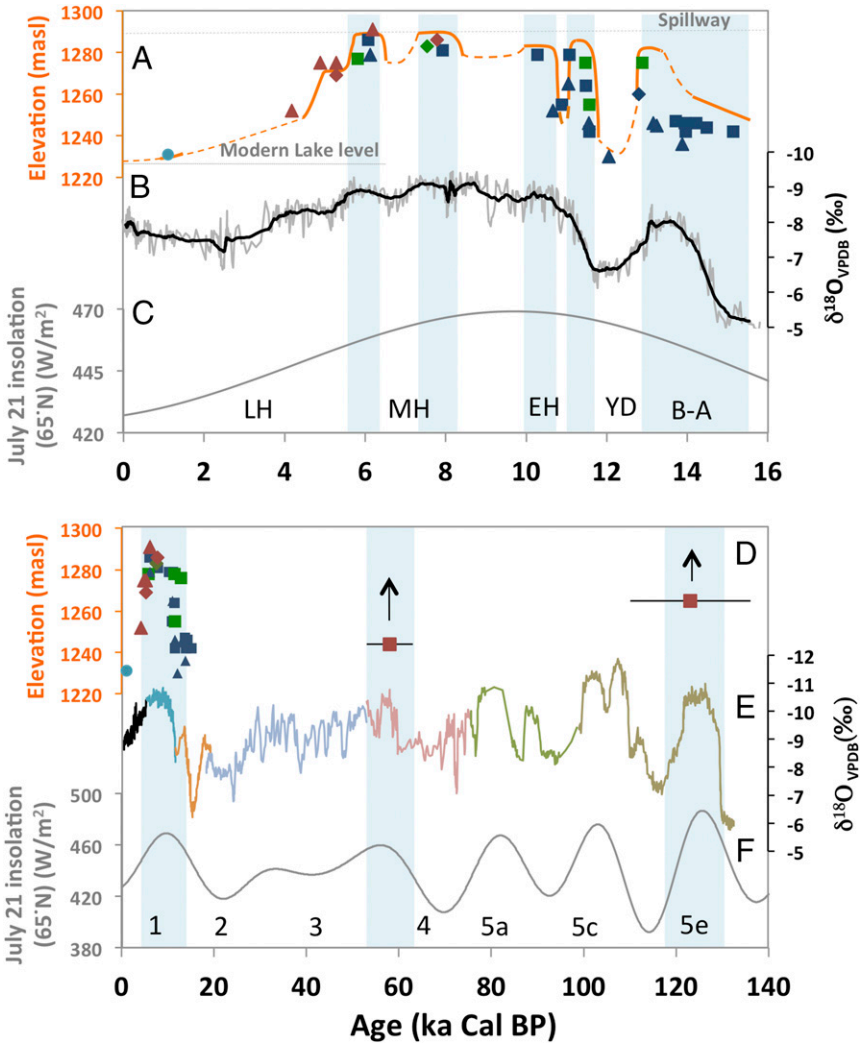

Fig. 2. Lake level reconstruction. (*A*) Lake Dali level for the past 16 ka, lake sediments (square), alluvial deposits (triangle), and beach ridges (diamond) were dated using ^{14}C from shell (blue), ^{14}C from charcoal (green), and OSL (red). In situ shell layers deposited in the swash zone indicate shoreline proximity; shells found in secondary deposition within alluvial sediments indicate lake level was higher than the elevation the shells were eroded into (*SI Materials and Methods*; Tables S2–S4). The lowest section of the Jin Wall indicates an upper limit for lake level (turquoise circle). Dashed orange lines represent times when the magnitude of lake level change is uncertain. (*B*) Oxygen isotope composition from Dongge Cave (19). (*C*) North hemisphere summer (July 21) insolation at 65°N (2, 31). (*D*) Same as *A* for the past 140 ka. (*E*) Compiled oxygen isotope composition of the Chinese cave deposits (light blue is from Hulu Cave; all other colors are different stalagmites from Sanbao Cave) (2). (*F*) Same as *C* for the past 140 ka.

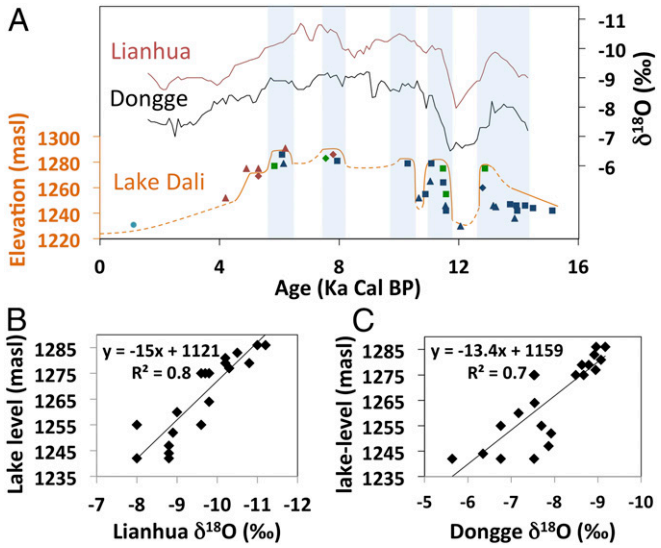

Fig. 3. Lake Dali lake level vs. cave $\delta^{18}O_c$. (*A*) Smoothed $\delta^{18}O_c$ Lianhua (red curve, 5-point average) and Dongge (black, 10-point average), and Lake Dali lake level (orange). (*B*) Correlation between Lianhua $\delta^{18}O_c$ and Lake Dali lake level. (*C*) Correlation between Dongge $\delta^{18}O_c$ and Lake Dali lake level. Light-blue bars represent highstands of the lake.

both north China lake (16) and sea surface temperature records (17); their cause is not clear at this time.

Discussion

The main point of contention over the interpretation of the Chinese cave deposit isotope records is whether the isotopic composition of precipitation in China (δ_P) is correlated with the amount of local rainfall over China. To evaluate whether the Chinese cave deposits represent actual rainfall amounts, we compare the Lake Dali record to two cave deposit records from north (Lianhua Cave located ~600 km south of Lake Dali; ref. 18) and south China (Dongge Cave located ~1,500 km south of Lianhua Cave; ref. 19; Fig. 1).

The results show that Lake Dali lake-level history is negatively correlated with both cave records on both precessional and millennial time scales (r^2 = 0.8 and 0.7 for Lianhua and Dongge, respectively) (Fig. 3 and Fig. S3). High Dali lake levels correspond with depleted Chinese cave deposits isotopic compositions and vice versa. These results indicate that to first order, the isotopic composition of precipitation is correlated with local rainfall amount over northern China and that both are regulated by EAM intensity.

The great advantage of closed-basin lakes is the quantitative constrains they can provide on paleo-rainfall amounts through a lake hydrological model. At equilibrium (stable lake level), the amount of water evaporating from the lake surface matches the inflow into the lake, which is calculated as the fraction of precipitation in the catchment that enters the lake as runoff multiplied by the catchment area of the lake and precipitation amount (20). To constrain the model, we first investigated the modern lake using satellite imagery, lake and stream chemistry, and long-term measurements of precipitation, air temperature, and evaporation (*SI Materials and Methods*). The results show that modern Lake Dali is a closed-basin lake at steady state, which allows us to use a closed-basin lake model and derive the essential modern hydrological parameters (e.g., lake evaporation and fraction of runoff).

To model the paleohydrology of the lake during the Holocene humid period and during the B–A, we used a digital elevation model to reconstruct the area of the lake based on the reconstructed lake level and a range of plausible lake evaporation rates using the Penman evaporation equation (21) and temperature reconstructions from the Chinese Sea (22) and climate models (23). To constrain the fraction of catchment runoff that enters the lake we used the Budyko relationship, which is an empirical model that relates the runoff fraction (rainfall/runoff) with precipitation amounts (24, 25). Our results show that annual precipitation during the early Holocene highstands must have been about double the present value for this lake basin (Fig. 4*A*). Because the lake likely overflowed during this time, this value

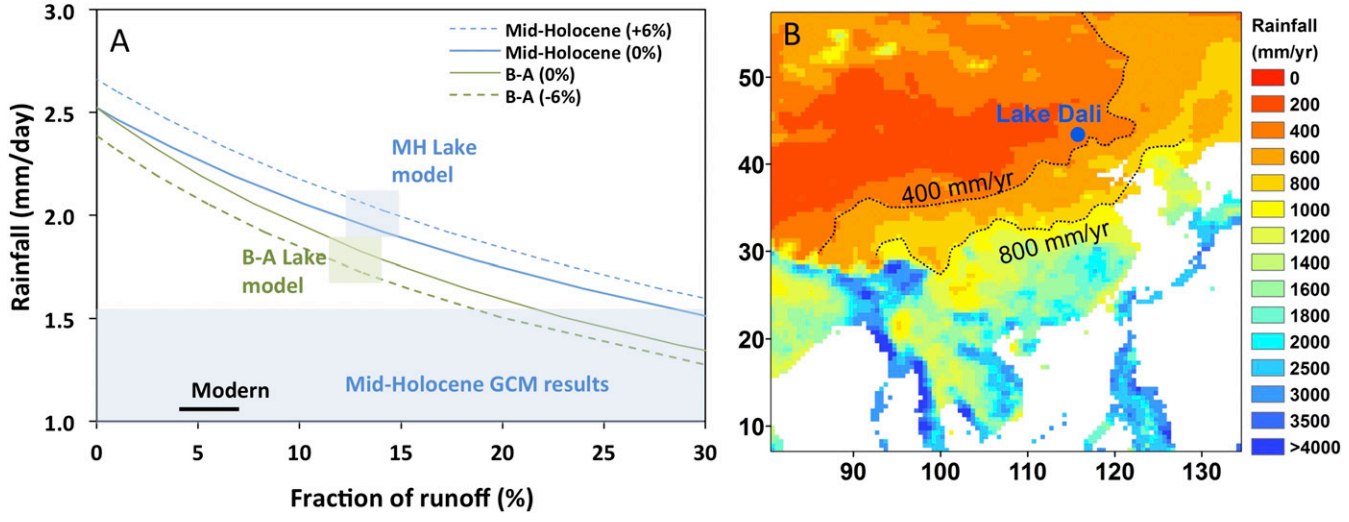

Fig. 4. Rainfall reconstructions. (*A*) The Holocene humid period (blue lines) and B–A (green lines) hydrologic scenarios calculated using a combination of a closed-basin lake model with the Budyko relation between precipitation amount and runoff fraction (blue and green shaded squares). The solid lines are for no change in evaporation rate, and the dashed lines include changes in evaporation rate calculated using the Penman equation (*SI Materials and Methods*). The range of general circulation model (GCM) precipitation values for the Mid-Holocene humid period is shown in the shaded blue band (*SI Materials and Methods*; Table S5). The modern rainfall and fraction of runoff is shown for comparison (black line). (*B*) East Asian modern rainfall distribution (shaded) (data from the Global Precipitations Climatology Centre, www.esrl.noaa.gov/psd/data/gridded/data.gpcc.html). A doubling of rainfall during the Early and Middle Holocene (from 400 to 800 mm/y) requires an ~400 km northward shift of the 800 mm isohyet.

should be regarded as a minimum estimate. Sustaining the B–A lake level would require 160–170% of modern precipitation values (Fig. 4*A*; *SI Materials and Methods*). Based on the modern spatial distribution of rainfall in China, a doubling of rainfall (from 400 to 800 mm/y) would require an ∼400 km northwestern movement of the 800-mm/y isohyet (Fig. 4*B*). Higher lake levels during the B–A, Middle and Early Holocene are most likely the outcome of two processes, the overall intensification of the EAM (as represented by the Chinese cave records), and a northwestern expansion of the monsoon. Assessing the proportional contribution of both processes is not possible at this time due to the lack of quantitative rainfall reconstructions from the central region of the EAM.

We compared our reconstructions of precipitation amount and the inferred northward extension of the EAM during the Holocene humid period to the 6-ka simulations from 12 paleoclimate modeling intercomparison project phase 3 (PMIP3) and National Center for Atmospheric Research (NCAR) general circulation models. Eleven of thirteen models accurately capture the northwestward EAM expansion. However, annual precipitation estimates from these simulations underestimate the magnitude of northern China hydrological change by 50% (Fig. 4) (see *SI Materials and Methods*, Fig. S4, Table S5, and ref. 26 for similar conclusions).

Our results suggest the abrupt termination of the Holocene humid period at 5.5–5 ka had dramatic impacts on the social development of Chinese culture. At this time, a major cultural transition occurred in north and central China identified by the disappearance of Early Neolithic cultures (Hongshan culture in North China, which existed from 6.5 to 5 ka, and Yangshao culture in central China which existed from 7 to 5 ka) (27). In central China, Early Neolithic cultures were replaced by stratified and socially and politically complex Late Neolithic cultures (e.g., Longshan culture that existed from 5 to 3.9 ka) (27), and previously unoccupied areas on the eastern margin of the Tibetan plateau were populated (28). In contrast, northeast China experienced a sharp population decline represented by the Xiaoheyan culture, which existed between 5 and 4.2 ka (27, 29). The sharp decline of north China rainfall amounts as recorded in Lake Dali, may have triggered contrasting reorganizations of north and central China cultures, causing a rapid population collapse in northern China and promoting structured complex societies in central China.

Materials and Methods

Lake beach ridges identified using satellite images and an ASTER digital elevation model were mapped in the field; stratigraphic relations were evaluated and samples were collected for dating.

Thirty-six shell and charcoal samples were dated using conventional radiocarbon methods. Analysis of modern lake water samples showed that there is no old radiocarbon in the lake. Nine sediment samples were dated using conventional OSL methods.

The hydrological model combines a closed-basin mass balance equation with the Budyko relationship, which is an empirical model that relates runoff fraction with precipitation amount and the Penman equation to quantify lake evaporation. The percent rainfall increase between modern and lake highstand, calculated using the hydrological model, was compared with the 6-ka simulations from 12 PMIP3 and NCAR general circulation models.

SI Materials and Methods contains a detailed description of sampling, dating, hydrological modeling, and comparison of the lake level with the ice-volume corrected $\delta^{18}O_c$ from the Chinese cave records.

ACKNOWLEDGMENTS. We thank G. Shelach-Lavi for his advice regarding the archaeology of China. We thank E. Sheng and T. Liu for their great help in the field. We thank the editor and two anonymous reviewers whose comments improved the paper. This work was supported by a Gary Comer Science and Education Foundation grant to Y.G. and P.J.P.; Columbia's Center for Climate and Life; the National Basic Research Program of China Grant 2013CB955900; the External Cooperation Program of Bureau of International Cooperation, Chinese Academy of Sciences Grant 132B61KYSB20130003; and Lamont–Doherty Earth Observatory Contribution no. 8084.

1. An Z, et al. (2000) Asychronous Holocene optimum of the East Asian monsoon. *Quat Sci Rev* 19:743–762.
2. Wang Y, et al. (2008) Millennial- and orbital-scale changes in the East Asian monsoon over the past 224,000 years. *Nature* 451(7182):1090–1093.
3. Liu Z, et al. (2014) Chinese cave records and the East Asia Summer Monsoon. *Quat Sci Rev* 83:115–128.
4. Orland IJ, et al. (2015) Direct measurements of deglacial monsoon strength in a Chinese stalagmite. *Geology* 43(6):555–558.
5. Maher BA (2008) Holocene variability of the East Asian summer monsoon from Chinese cave records: A re-assessment. *Holocene* 18(6):861–866.
6. Pausata FSR, Battisti DS, Nisancioglu KH, Bitz CM (2011) Chinese stalagmite $\delta^{18}O$ controlled by changes in the Indian monsoon during a simulated Heinrich event. *Nat Geosci* 4(7):474–480.
7. Lee J-E, et al. (2012) Asian monsoon hydrometeorology from TES and SCIAMACHY water vapor isotope measurements and LMDZ simulations: Implications for speleothem climate record interpretation. *J Geophys Res* 117(D15):D15112.
8. Battisti DS, Ding Q, Roe GH (2014) Coherent pan-Asian climatic and isotopic response to orbital forcing of tropical insolation. *J Geophys Res Atmos* 119(21):11997–12020.
9. Caley T, Roche DM, Renssen H (2014) Orbital Asian summer monsoon dynamics revealed using an isotope-enabled global climate model. *Nat Commun* 5:5371.
10. Chiang JCH, et al. (2015) Role of seasonal transitions and westerly jets in East Asian paleoclimate. *Quat Sci Rev* 108:111–129.
11. An Z, et al. (2015) Global monsoon dynamics and climate change. *Annu Rev Earth Planet Sci* 43:29–77.
12. Street-Perrott FA, Harrison SP (1985) Lake levels and climate reconstruction. *Paleoclimate Data and Modeling*, ed Hecht AD (John Wiley, New York), pp 291–340.
13. Yu G, Ke X (2007) Lake level studies/Asia. *Encyclopedia of Quaternary Science*, ed Scott AE (Elsevier, Amsterdam), Vol 2, 1st Ed, pp 1343–1359.
14. Bureau of Geology and Mineral Resources of Nei Mongol Autonomous Region (1991) *Regional Geology of Nei Mongol (Inner Mongolia) Autonomous Region. Geological Memoirs, Series 1* (Geology Publishing House, Beijing).
15. Broecker W, Putnam AE (2012) How did the hydrologic cycle respond to the two-phase mystery interval? *Quat Sci Rev* 57:17–25.
16. Schettler G, et al. (2006) East-Asian monsoon variability between 15,000 and 2000 cal. yr BP recorded in varved sediments of Lake Sihailongwan (northeastern China, Long Gang volcanic field). *Holocene* 8:1043–1057.
17. Kubota Y, et al. (2010) Variations of East Asian summer monsoon since the last deglaciation based on Mg/Ca and oxygen isotope of planktic foraminifera in the northern East China Sea. *Paleoceanography* 25(4):PA4205.
18. Dong J, Shen C, Kong X, Wang H, Jiang X (2015) Reconciliation of hydroclimate sequences from the Chinese Loess Plateau and low-latitude East Asian Summer Monsoon regions over the past 14,500 years. *Palaeogeogr Palaeoclimatol Palaeoecol* 435: 127–135.
19. Dykoski CA, et al. (2005) A high-resolution, absolute-dated Holocene and deglacial Asian monsoon record from Dongge Cave, China. *Earth Planet Sci Lett* 233(1-2):71–86.
20. Broecker WS, Putnam AE (2013) Hydrologic impacts of past shifts of Earth's thermal equator offer insight into those to be produced by fossil fuel CO2. *Proc Natl Acad Sci USA* 110(42):16710–16715.
21. Penman HL (1948) Natural evaporation from open water, hare soil and grass. *Proc R Soc Lond A Math Phys Sci* 193(1032):120–145.
22. Sun Y, Oppo DW, Xiang R, Liu W, Gao S (2005) Last deglaciation in the Okinawa Trough: Subtropical northwest Pacific link to Northern Hemisphere and tropical climate. *Paleoceanography* 20(4):PA4005.
23. Braconnot P, et al. (2007) Results of PMIP2 coupled simulations of the Mid-Holocene and Last Glacial Maximum. Part 1: Experiments and large-scale features. *Clim Past* 3(2):261–277.
24. Budyko MI (1974) *Climate and Life* (Academic, San Diego).
25. Koster RD, Fekete BM, Huffman GJ, Stackhouse PW (2006) Revisiting a hydrological analysis framework with International Satellite Land Surface Climatology Project Initiative 2 rainfall, net radiation, and runoff fields. *J Geophys Res* 111(D22):1–12.
26. Harrison SP, et al. (2015) Evaluation of CMIP5 palaeo-simulations to improve climate projections. *Nat Clim Chang* 5(8):735–743.
27. Shelach-Lavi G (2015) *The Archaeology of Early China: From Prehistory to the Han Dynasty* (Cambridge Univ Press, New York).
28. Guedes A (2015) Rethinking the spread of agriculture to the Tibetan Plateau. *Holocene* 25(9):1498–1510.
29. Shelach-Lavi G, et al. (2016) Human adaptation and socio-economic change in Northeast China: Results of the Fuxin Regional Survey. *J Field Archaeol* 41(4):467–485.
30. An Z, Sun Y, Chang H, Zhang P, Liu X (2014) *Late Cenozoic Climate Change in Monsoon-Arid Asia and Global Changes* (Springer, Dordrecht).
31. Berger AL (1978) Long-term variations of caloric insolation resulting from the earth's orbital elements. *Quat Res* 9(2):139–167.
32. Yang X, Ding Z, Fan X, Zhou Z, Ma N (2007) Processes and mechanisms of desertification in northern China during the last 30 years, with a special reference to the Hunshandake Sandy Land, eastern Inner Mongolia. *Catena* 71(1):2–12.
33. Ding Y, Wang Z, Sun Y (2008) Inter-decadal variation of the summer precipitation in East China and its association with decreasing Asian summer monsoon. Part I: Observed evidences. *Int J Climatol* 28(9):1139–1161.

34. Santos GM, Southon JR, Griffin S, Beaupre SR, Druffel ERM (2007) Ultra small-mass AMS 14C sample preparation and analyses at KCCAMS/UCI Facility. *Nucl Instrum Meth B* 259(1):293–302.
35. Zhou W, et al. (2007) New results on Xi'an-AMS and sample preparation systems at Xi'an-AMS center. *Nucl Instrum Meth B* 262(October 2006):135–142.
36. Stuvier M, Polach HA (1977) Reporting of 14C Data. *Radiocarbon* 19(3):355–363.
37. Bronk RC (1995) Radiocarbon calibration and analysis of stratigraphy: The OxCal program. *Radiocarbon* 37(2):425–430.
38. Bronk RC (2001) Development of the radiocarbon program OxCal. *Radiocarbon* 43(2A):355–363.
39. Wang YJ, et al. (2001) A high-resolution absolute-dated late Pleistocene Monsoon record from Hulu Cave, China. *Science* 294(5550):2345–2348.
40. Prescott J, Hutton J (1994) Cosmic ray contributions to dose rates for luminescence and ESR dating: Large depths and long-term time variations. *Radiat Meas* 23: 497–500.
41. Fairbanks RG (1989) A 17,000-year glacio-eustatic sea level record: Influence of glacial melting rates on the Younger Dryas event and deep-ocean circulation. *Nature* 342(6250):637–642.
42. Schrag DP, et al. (2002) The oxygen isotopic composition of seawater during the Last Glacial Maximum. *Quat Sci Rev* 21(1-3):331–342.
43. Kim S-T, O'Neil JR (1997) Equilibrium and nonequilibrium oxygen isotope effects in synthetic carbonates. *Geochim Cosmochim Acta* 61(16):3461–3475.
44. Liu B (2004) A spatial analysis of pan evaporation trends in China, 1955–2000. *J Geophys Res* 109(D15):D15102.
45. Linacre ET (1994) Estimating U.S. class A pan evaporation from few climate data. *Water Int* 19(1):5–14.
46. Yang X, et al. (2013) Initiation and variation of the dune fields in semi-arid China - With a special reference to the Hunshandake Sandy Land, Inner Mongolia. *Quat Sci Rev* 78:369–380.
47. Yang X, et al. (2008) Late Quaternary environmental changes and organic carbon density in the Hunshandake Sandy Land, eastern Inner Mongolia, China. *Glob Plan Change* 61(1-2):70–78.
48. Zhang H, Tian M, Guo J, Yang J (2012) The dynamic monitoring of Dalinur Lake in Inner Mongolia during 1999-2010 based on RS and GIS. *J Arid L Resour Environ* 26(10): 41–46.